Proceedings of the 30th International Cosmic Ray Conference
Rogelio Caballero, Juan Carlos D'Olivo, Gustavo Medina-Tanco,
Lukas Nellen, Federico A. Sánchez, José F. Valdés-Galicia (eds.)
Universidad Nacional Autónoma de México,
Mexico City, Mexico, 2008

Vol. 3 (OG part 2), pages 1241–1244

30TH INTERNATIONAL COSMIC RAY CONFERENCE

Radiofrequency Ice Properties Measurements at Taylor Dome, Antarctica, in support of the ANITA experiment

D. Z. BESSON[1], J. NAM[2], S. MATSUNO[3], S. W. BARWICK[2], J. J. BEATTY[4], W. R. BINNS[5], C. CHEN[6], P. CHEN[6], J. M. CLEM[7], A. CONNOLLY[8], P. F. DOWKONTT[5], M. A. DUVERNOIS[9], R. C. FIELD[6], D. GOLDSTEIN[2], A. GOODHUE[8] P. W. GORHAM[3], C. HAST[6], C. L. HEBERT[3], S. HOOVER[8], M. H. ISRAEL[5], J. KOWALSKI,[3] J. G. LEARNED[3], K. M. LIEWER[10], J. T. LINK[1,11], E. LUSCZEK[9], B. MERCURIO[4], C. MIKI[3], P. MIOČINOVIĆ[3], C. J. NAUDET[10], J. NG[6], R. NICHOL[4], K. PALLADINO[4], K. REIL[6], A. ROMERO-WOLF[1] (*presenter*), M. ROSEN[3], L. RUCKMAN[3], D. SALTZBERG[8], D. SECKEL[7], G. S. VARNER[3], D. WALZ[6], F. WU[2].

[1]*Dept. of Physics and Astronomy, Univ. of Kansas, Lawrence, KS 66045.* [2]*Univ. of California, Irvine CA 92697.* [3]*Dept. of Physics and Astronomy, Univ. of Hawaii, Manoa, HI 96822.* [4]*Dept. of Physics, Ohio State Univ., Columbus, OH 43210.* [5]*Dept. of Physics, Washington Univ. in St. Louis, MO 63130.* [6]*Stanford Linear Accelerator Center, Menlo Park, CA, 94025.* [7]*University of Delaware, Newark, DE 19716.* [8]*Dept. of Physics and Astronomy, Univ. of California, Los Angeles, CA 90095.* [9]*School of Physics and Astronomy, Univ. of Minnesota, Minneapolis, MN 55455.* [10]*Jet Propulsion Laboratory, Pasadena, CA 91109.* [11]*Currently at NASA Goddard Space Flight Center, Greenbelt, MD, 20771.*

dbesson@ku.edu

Abstract: Radiowave detection of the Cherenkov radiation produced by neutrino-ice collisions requires an understanding of the radiofrequency (RF) response of cold polar ice. We herein report on a series of radioglaciological measurements performed approximately 10 km north of Taylor Dome Station, Antarctica from Dec. 6, 2006 – Dec. 16, 2006. Using RF signals broadcast from a dual-polarization horn antenna on the surface transmitting signals which reflect off the underlying bed and back up to a dual polarization surface horn receiver, we have made time-domain estimates of both the real (index-of-refraction "n") and imaginary (attenuation length "L_{atten}") components of the complex ice dielectric constant ($\epsilon = \epsilon' + i\epsilon''$). We have also measured the uniformity of ice response along two orthogonal axes in the horizontal plane. We observe an apparent wavespeed asymmetry of order 0.1%, between two orthogonal linear polarizations projected into the horizontal plane, consistent with some previous measurements, but somewhat lower than others.

Introduction

The radiofrequency transparency of cold ice allows a radio sensor to probe an extremely large volume for englacially generated radiowave signals. In the case where ultra-high energy cosmic-ray neutrinos are measured via the coherent Cherenkov radiation produced subsequent to their collision with ice molecules, ice properties must be understood to estimate the neutrino flux sensitivity. Measurement of Antarctic ice properties over a large footprint is particularly important for the ANITA experiment[1], which seeks to register neutrino-induced radiowave signals using a suite of high-bandwidth horn antennas mounted on a gondola. From a height of 38 km, ANITA monitors a mass of ice out to the horizon 680 km away. Data from a successful flight in Dec. 2006 – Jan. 2007 is now being scrutinized for evidence of neutrino interactions.

In principle, ground-penetrating radar can be used to probe ice dielectric properties. A continuous wave (CW) network analyzer signal, fed into a Transverse ElectroMagnetic (TEM) horn, can be used to excite one particular polarization[2]. If that signal polarization axis is aligned with one of the linear birefringence axes (aka "optical axes", or "ordinary" and "extraordinary" axes), no bire-

fringent asymmetry is observed. In the case where the signal polarization axis projects onto two orthogonal birefringence axes, a birefringent asymmetry ($\delta_{\epsilon'} \neq 0$) in the real part of dielectric constant will result in interference between the two orthogonal signals arriving at the receiver, with some frequency and pathlength-dependent reduction in observed signal magnitude. This technique has been used in the past to probe ice birefringent effects near Dome Fuji, e.g[3].

As an alternative to frequency-domain measurements, one can directly measure asymmetries in the time domain using a pulsed signal. This approach has the disadvantage of obscuring the frequency dependence of the signal propagation, but the advantage of isolating through-air signal leakage due to the side lobes of a typical horn beam pattern and/or other possible multi-path effects. In this case, $\delta_{\epsilon'} > 0$ results in a measurable time difference between two signal polarizations; $\delta_{\epsilon''} > 0$ results in an amplitude difference between two polarizations.

Geometry

The geography of the ITASE drill site where these measurements were conducted near Taylor Dome is presented in Figure 1. This site is approximately 100 km. East of McMurdo Station, at an elevation of approximately 2 km. Two large bandwidth TEM dual-polarization horns, identical to those used on the ANITA gondola were used for the measurements described herein. For reflection off the underlying bedrock, the orientation of the surface horn antennas is specified by the two orthogonal linear polarization 'V' and 'H' axes. In the case where both transmitter ("Tx") and receiver ("Rx") are aligned with 'V', the orientation is therefore described as 'VV', e.g. For the in-ice measurements described below, the VV-axis is approximately 14.8 degrees East of true North, and points roughly in the direction of the primary Taylor Dome base. Over a distance scale of $\sim$10 km, the VV axis approximately coincides with the local surface elevation gradient. Locally (over $\sim$0.5 km), the HH-axis coincides roughly with the local gradient.

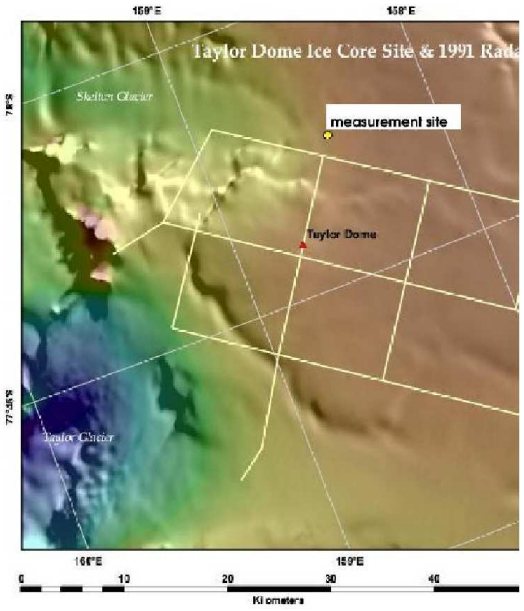

Figure 1: Coordinates of measurement site (yellow circle) and main Taylor Dome base (red triangle)

Received Power Magnitude and L_{atten}

Two complementary calculations permit an estimate of the average ice radiofrequency electric field attenuation length (L_{atten}) at our site. First, we compare the signal strength measured through the in-ice path (S_{12}(ice)) normalized relative to the signal strength measured when the transmitting horn broadcasts along boresight to the receiver horn in-air (S_{12}(air)). Knowing the distance between the horns in-air (d_{air}) and the round-trip distance of the signal path through ice d_{ice}, and attributing all losses greater than (assumed spherical) 1/r amplitude spreading to ice attenuation, we can use $V_{ice}/V_{air} = (G_{air}/G_{ice}) \times (d_{air}/d_{ice})e^{-d_{ice}/\langle L_{atten}\rangle}$ to extract the mean field attenuation length $\langle L_{atten}\rangle$, with G the antenna gains and V_{ice} and V_{air} the measured voltages for the in-ice and in-air signal paths, respectively. Second, we 'absolutely' normalize the received signal using the Friis radar equation[4].

Assumption-dependent numerical results for our pathlength-averaged attenuation length are presented in Table 1. Results are presented for a vari-

ety of assumptions regarding the coherence of the signal at the bedrock, as well as the reflection coefficient at the bedrock interface. The long duration of the observed reflection indicates incoherent basal scattering (Figure 2).

Table 1: Summary of attenuation length measurements, under various assumptions for the reflection coefficient and the coherence characteristics of the underlying bedrock. Values shown are averaged over multiple measurements. Errors represent statistical spread of calculated values only. $\mathcal{R}$ denotes the assumed bedrock reflectivity, $\int t_{refl}$ denotes the time duration of the assumed reflected signal.

$\mathcal{R}$	Signal Norm.	Basal Scattering	$\int t_{refl}$	$\langle L_{atten} \rangle$ (m)
1.0	In-air	Coherent	10 ns	340 ± 15
1.0	In-air	Coherent	50 ns	351 ± 15
1.0	In-air	Coherent	250 ns	616 ± 32
1.0	In-air	Incoherent	10 ns	441 ± 25
1.0	In-air	Incoherent	50 ns	458 ± 26
1.0	In-air	Incoherent	250 ns	1055 ± 95
1.0	Friis	Incoherent	250 ns	628
0.3	Friis	Incoherent	250 ns	1051

Experimental Comparison of Bottom Reflection signals

Bottom reflection data were taken in "VV", "HH", and "VH" orientations. The start times (t_0) from the pulser for our measurements are found to be identical to within ∼200 ps.

Comparing "HH" to "VV" reflections, we observe that the echo time recorded for the "HH" signal is advanced by 15 ns relative to the "VV" echo signal time (Figure 2). Aside from the unlikely possibility that the bottom surface has local 'patches' which favor different polarizations, it would appear that the most likely explanation for this observed time difference is due to wavespeed differences along two axes. Interpreted as birefringence, the implied asymmetry is approximately 0.12%. Although not fully probed owing to time and cable length limitations, and also problems with data acquisition waveform capture we note that the magnitude of the HH vs. VV signals were relatively constant when the receiver antenna was displaced along the

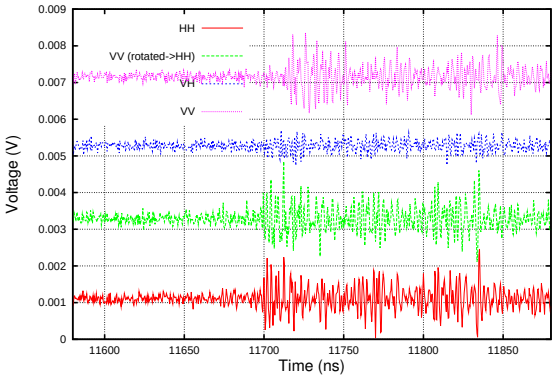

Figure 2: Received signal as a function of time for indicated orientations. "VV→HH rotate" refers to the Tx and Rx orientation for which the VV axes of both Tx and Rx have been rotated into the initial HH orientation. In this (and successive) Figures, the three uppermost signals have been vertically offset to enhance visual clarity.

N-S axis by approximately 170 m (in that case, the illuminated area of bedrock at which the reflection is taking place should be displaced by ∼85 m) and then rotated in 22.5 degree steps over 180 degrees. The intent here was to probe the specular component of the surface scattering and attempt to discern variations in peak receiver voltage, as a function of orientation. The measured values of peak receiver voltage, read off the TDS694C oscilloscope screen connected to the receiver horn, are presented in Figure 3. We observe from Figure 3 that: a) our initial "VV" orientation of –14.8 degrees seems to be close to the measured maximum; b) from interference effects, and assuming that the birefringent asymmetry in the real part of the dielectric constant is substantially larger than in the imaginary component, we would naively expect maxima at intervals of $\pi/2$, corresponding to those orientations for which the antenna polarization axis is aligned with either of the optical axes; c) absent physical effects which rotate the polarization plane of the propagating signal, we would expect the received cross-polarization ($V \rightarrow H$, e.g.) fraction of the received signal to be approximately constant. The largeness of the point-to-point systematic errors and the lack of comprehensive data notwithstanding, such constancy is not obviously observed. Rather, there ap-

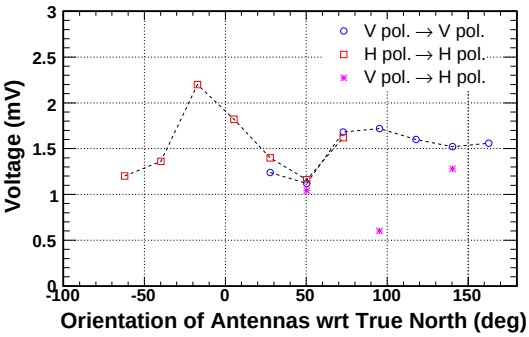

Figure 3: Maximum measured bottom reflection voltage (as read directly from oscilloscope) with surface receiver horn displaced 150 m south of initial measurements. Typical measurement uncertainty is estimated to be of order 20% at each point. "Negative" corresponds to a clockwise rotation from true North; i.e., in the direction towards East.

pears to be an anti-correlation between "co-pol" (VV or HH) signal strength and cross-pol (VH) signal strength – when the former is largest, the latter is smallest, and vice versa.

To check antenna systematics, the surface horn transmitter and surface horn receiver were rotated in the horizontal plane by –90 degrees; in that configuration, we find HH(rotated)=VV(unrotated), and VV(rotated)=HH(unrotated). This indicates that the observed time-domain asymmetry is not an artifact of antenna effects.

Summary

Our model-dependent attenuation length estimates are, given the large errors, consistent with previous measurements at the South Pole[5]. Our birefringence measurements are also consistent with other estimates[6, 7, 8]. The quantitative impact of any possible birefringence will depend on the experimental details of a given data acquisition system and the location-specific ice properties. For the ANITA experiment, the effect is expected to be negligible, since the data acquisition system integrates $\sim$8 ns after the initial trigger signal, and also since almost all the detected neutrino flux corresponds to the case where the Cherenkov electric-field vector is polarized predominantly in the vertical plane, whereas birefringence should be most noticeable for the case where the $\vec{E}$ polarization vector coincides with one of the principal axes of the ice crystal (assumed to be oriented horizontally, in the case where the fabric is defined by the horizontal ice flow). Additionally, the bulk of the sensitive volume probed by ANITA is slower-moving, thicker interior ice, for which birefringent effects are expected to be somewhat smaller than near the continental periphery.

Acknowledgments

We thank RPSC and the National Science Foundation Office of Polar Programs for their excellent logistical support. ANITA is supported under NASA Grant NAG5-5387. Jessy Jenkins and Matt Smith directed and oversaw establishment of the field camp. The ITASE collaboration drilled the borehole used for many of these measurements.

References

[1] K. Palladino *et. al.* (The ANITA Collaboration), paper 1095, submitted to these proceedings.
[2] S. Fujita et. al., J. Glaciol. 52 (178), 407 (2006).
[3] K. Matsuoka et. al., J. Glaciol. 50 (170), 382 (2004).
[4] C. Balanis, *Antennas, Theory Analysis and Design*, 2nd Ed., (1982)
[5] S. Barwick et. al., J. Glaciol. 04J067 (2005).
[6] N. D. Hargreaves, J. Glaciol. 21, 301-313, 1978.
[7] K. Matsuoka et. al., J. Geophys. Res., 108 (B10), 2003.
[8] C. Doake et al., Ann. of Glaciol., (34) 1, 2002.